Feedforward Linearization of Analog Modulated Laser Diodes—Theoretical Analysis and Experimental Verification

D. Hassin and R. Vahldieck, *Senior Member, IEEE*

Abstract—**This paper discusses feedforward linearization of directly modulated laser diodes for AM CATV lightwave transmission systems. Theoretical simulation and experimental results are presented showing a distortion cancellation of better than 20 dB over 850 MHz bandwidth. An investigation regarding tolerance and possible dispersion penalty in the system is performed. A noise analysis is presented including the theoretical examination of laser relative intensity noise (RIN) reduction by feedforward compensation.**

I. Introduction

FIBER-OPTIC transmission of CATV signals promises many advantages over coaxial-based systems mainly due to the high bandwidth of optical transmitters and low losses of fiber. However, the AM-VSB signal format used for CATV requires a carrier to noise ratio (CNR) near 50 dB for good picture quality. In addition, the many distortion products generated by system nonlinearities must have a cumulative power (composite second order distortion) CSO and composite triple beat (CTB) that is more than 60 dB below the carrier level. Meeting these requirements using AM lightwave systems has proven to be feasible, but difficult in view of the fact that a sensitive compromise exists between CNR and linearity. This tradeoff can be eased by employing various linearization schemes. In order for these schemes to be effective, however, optical sources with sufficient power and low noise must be employed to satisfy simultaneously CNR and power budget specifications. In this paper we discuss the potential of feedforward linearization [2] of directly modulated optical transmitters with respect to channel capacity (60–150), dispersion penalty and RIN cancellation. Although for a lower number of channels, state of the art commercially available single laser diodes can satisfy the strict CSO, CTB, and CNR requirements demanded by CATV operators, this is in most cases not possible without some kind of predistortion (i.e., [12]). Predistortion, on the other hand, has had only limited success since the predistortion network must be matched to the individual laser and must take into account the strong frequency dependent distortion generated by semiconductor laser diodes. Laser aging and other undesired effects may deteriorate the performance of a predistortion network. Alternatively, quasi-feedforward linearization schemes (i.e., [11]) require matched lasers to be effective, but matched laser diodes are very difficult to obtain.

Therefore, we consider the feedforward linearization, although a relatively complicated and sensitive scheme, as a promising linearization solution especially in view of the demand for high channel capacity lightwave systems. Feedforward linearization was reported in [2], [8]. However, the published results left open a number of questions concerning the maximum number of channels possible, the maximum possible cancellation of third harmonic and third order intermodulation distortion, the impact of tolerances in the feedforward scheme as well as fiber dispersion on the effectiveness of the linearization, and to what degree noise cancellation can be achieved without jeopardizing the linearization effect. The following is an attempt to fill in the gap and to provide more insight into the potential as well as limitations of this linearization scheme.

II. Feedforward Linearization

A simplified feedforward circuit diagram is illustrated in Fig. 1. The input signal is split into two paths; one of them modulates the primary laser (L1) while the other one is used as a reference signal. Detecting the signal out of L1 and comparing it with the time delayed original signal provides an error signal which is amplified and modulates the secondary laser (L2). The modulated optical signal from laser L2 combines with the optical signal of laser L1 and cancels the distortion products.

Before experimenting with this scheme to test the degree of distortion cancellation possible, we have developed a computer model to analyze its potential and to identify the system elements most critical for good performance. The most important factor in accurate modeling of such a system is the laser diode itself.

Manuscript received February 9, 1993; revised June 25, 1993. This work was funded by Canadian Cable Labs, Rogers Communications, Inc. and by the National Science and Engineering Research Council of Canada (NSERC).

The authors are with the Laboratory for Lightwave Electronics, Microwaves, and Communications (LLiMiC), Department of Electrical and Computer Engineering, University of Victoria, B.C., Canada, V8W # 3P6.

IEEE Log Number 9212955.

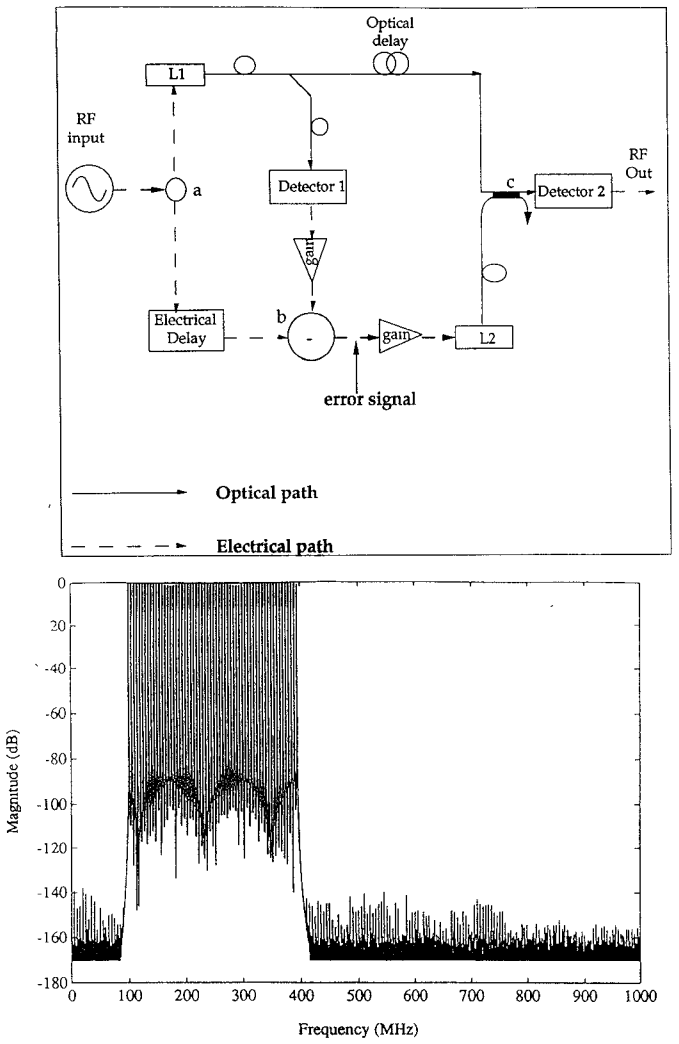

Fig. 1. Block diagram of the laser feedforward scheme and performance with 60 CATV channels.

Laser Diode Modeling

The basis for laser diode modeling are the laser's rate equations. Since the modulation frequencies in typical CATV applications are relatively low (currently < 1 GHz for AM-CATV), the package and chip parasitics are normally small enough as to not become a band-limiting factor. Hence, nonlinear laser distortion can be predicted accurately from the intrinsic laser model [3]–[6]. To become independent from equivalent network models for laser diodes, we have chosen to use the Volterra series analysis [1] of the laser rate equations. This approach enables us to perform small signal analysis, using a general and well defined mathematical treatment suitable for the description of weakly nonlinear systems. Our starting point in this analysis is the set of two coupled rate equations for a single mode laser. These equations describe the nonlinear interaction between injected carriers and photons in the laser cavity. Once the laser biasing point is well above threshold, the spontaneous process can be neglected with respect to the stimulated processes and the two rate equations can be combined to form a third equation, given by

$$I_a - I_{th} = \frac{V'}{\Gamma} \cdot \frac{dQ}{dt} + \frac{V'}{\Gamma \tau_p} \cdot Q + \frac{V'}{\Gamma g} \cdot \frac{d}{dt}\left\{ \frac{\frac{dQ}{dt} + \frac{Q}{\tau_p}}{(1 - \epsilon Q) Q} \right\}, \tag{1}$$

where I_a is the applied modulation current, I_{th} is the laser threshold current, V' is the volume of the active region times the electron charge, Γ is the optical confinement factor, Q is the photon density in the active region, τ_p is the photon life time, g is the optical gain factor, and ϵ is the gain compression parameter. The photon density is directly proportional to the laser optical output power. Since (1) relates the input modulating current to the photon density, it is regarded as an output to input connection [1]. The steady state solution of (1) (obtained by setting all time derivatives in (1) to zero) shows a completely linear relation between the dc part of the laser's optical output power and the input biasing current. This solution, however, applies only for dc quantities. Modeling of a nonlinear laser system is achieved by examining the ac (or time varying) part of (1). The time varying equation is given in Appendix A. It can be used to derive the first three transfer functions of an inverse laser system (a purely theoretical system for which the input is an alternating amount of optical power and the output is an alternating current) from which the first three complex transfer functions of a real laser system are obtained. Full expressions of these transfer functions are given in Appendix B. They show that the parameters of a given laser can be directly used to calculate its linear, second-order, and third-order transfer functions. Once the laser transfer function is known, a Volterra series analysis enables us to find the magnitude of any selective distortion term produced by the laser nonlinearity, as soon as its generating frequencies are specified. For example, the ratio of a second order intermodulation product of the type $\omega_1 - \omega_2$ with respect to the carrier, evaluated in the photodetector is given in dB by

$$\frac{IMD^{2'nd}}{C} = 20 \cdot 20 \log_{10}\left\{ m \cdot (I_{dc} - I_{th}) \cdot \frac{|H_2(\omega_1, -\omega_2)| \cdot |H_1(0)|}{|H_1(\omega_1)|^2} \right\}, \tag{2}$$

where I_{dc} is the laser's biasing current, m is the optical modulation index per tone, and H_1 and H_2 are the lasers linear and second-order transfer functions, respectively. In a similar way the ratio of a third-order intermodulation product of the type $2\omega_1 - \omega_2$, with respect to the carrier

(denoted as $IMD^{3'rd}$), is given in dB by

$$\frac{IMD^{3'rd}}{C} = 20 \cdot \log_{10}\left\{\frac{3}{4} \cdot m^2 \cdot (I_{dc} - I_{th})^2 \cdot \frac{|H_3(\omega_1, \omega_1, -\omega_2)| \cdot |H_1(0)|^2}{|H_1(\omega_1)|^3}\right\}. \quad (3)$$

H_3 is the laser's third-order transfer function.

Simulation of Feedforward Scheme

We have used our laser model to perform a frequency domain simulation of the feedforward linearization circuit shown in Fig. 1. Based on the results in [7], laser distortion as a result of a multichannel modulation signal was evaluated by summing the powers of all two-tone and three-tone intermodulation products that fall in a given frequency range.

Simulation results show that a reduction of 50 to 100 dB in composite nonlinear distortion can be achieved, depending on the lasers being utilized and the coupling ratio of the optical coupler at the circuit's output. This is because the main limiting factor in this scheme is the distortion introduced by the secondary laser, which is not compensated for. This distortion is minimized when L2 is driven by a relatively small signal. The magnitude of the signal modulating the secondary laser depends, among other parameters, on the optical coupling ratio at the output. For example, an optical power coupling ratio of 90 : 10 in favor of L1 dictates an input signal into L2 which is 9 times larger compared to the case of a coupling ratio of 50 : 50. An optical coupling ratio of 50 : 50, on the other hand, may be attractive since it provides an option for two linearized outputs from the optical transmitter. Thus, it might be possible to serve twice the number of subscribers by a single transmitter.

To demonstrate feedforward performance we will consider a 60 channel system with a modulation index of 4% per channel, employing relatively linear, but by no means best available lasers. An output coupling ratio of 50 : 50 was assumed. The lowest unlinearized distortion for a single laser was found to be −46 dBc. In comparison, simulation results for an ideal feedforward arrangement indicated a distortion reduction of about 92 dB to a level of −138 dB. This is illustrated in Fig. 1. Although in this simulation we have assumed two highly linear and low-noise lasers, which are costly in a practical setup, there is potential for employing low cost lasers which are less linear and exhibit higher RIN figures (i.e., [8]). A further advantage of this arrangement is that there is no need for both lasers to be similar. In fact, their optical wavelength must be different in order to prevent signal beats. The feedforward scheme was theoretically tested for a channel capacity of 40 to 150 channels. Results show that this linearization technique performs equally good for small as well as for a large number of channels. It is important to mention that the above results represent an "ideal case" analysis and should be regarded as the theoretical limit of the systems performance. Practical results were expected to be not as good, due to tolerance in the system, especially in the RF path. Therefore, a tolerance analysis is presented in the next section.

III. Tolerance and Dispersion Penalty Analysis

Device and component imperfections and tolerances encountered in the practical implementation of the system were taken into account in our simulation by adding four tolerance parameters to the "ideal case" simulation, presented above. These parameters are amplitude and phase errors between the two optical signals being combined at the circuit's output, and amplitude and phase errors between the two electrical signals being compared in the error signal generation. In general, all these parameters are frequency dependent. An analysis in the frequency domain enables us to directly use measured data from the vector network analyzer (VNA), in order to specify each error parameter over the circuit's bandwidth.

We have found that the systems performance is dominated by amplitude and phase match between the optical signals. Our simulations have shown that the maximum amount of nonlinear distortion reduction achievable in a practical system is about 30 dB. This requires an optical phase and amplitude match of less than 2 degrees and 0.5 dB, respectively. Such an accuracy is very difficult to obtain over a wide bandwidth. However, distortion reduction of more than 20 dB can be obtained if these strict tolerance conditions are eased to a phase and amplitude match of about 5 degrees and 1 dB, respectively.

We have also performed a theoretical investigation of a possible dispersion penalty in the system performance. This penalty is a result of a wavelength separation between the two lasers, followed by fiber chromatic dispersion which causes phase mismatch between the distorted signal out of laser L1 and the "corrective" signal from laser L2. The system can be optimized for maximum performance at a given transmission length in the fiber. A penalty will be encountered in case the actual transmission length is different. Fig. 2 shows the minimum linearization achievable for different fiber lengths of a system optimized for transmission through 0 km (practically a few meters) of fiber. It can be seen that dispersion penalty is more severe for high-bandwidth systems. This is due to the fact that a given dispersion induced-timing error translates into a larger phase mismatch at higher frequency signals. Fig. 3 shows the available linearization as a function of wavelength separation between the lasers. The system was optimized for a 10 km fiber length. It is evident that the more the emission wavelengths of both lasers differ, the effect of fiber dispersion deteriorates the system performance.

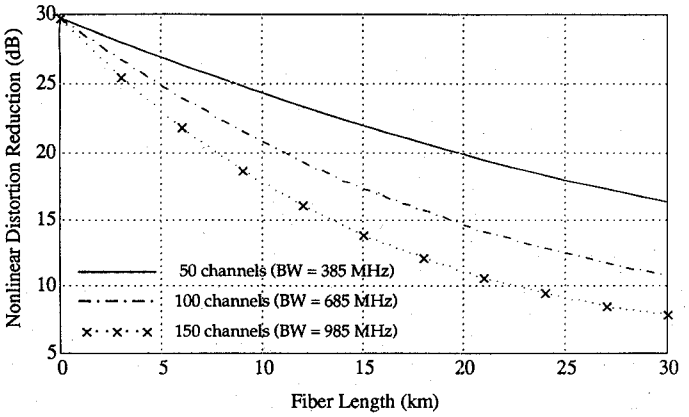

Fig. 2. Dispersion penalty as a function of fiber length. Wavelength separation between the two lasers = 2 nm. Fiber chromatic dispersion (at center wavelength) = 0.75 ps/nm · km.

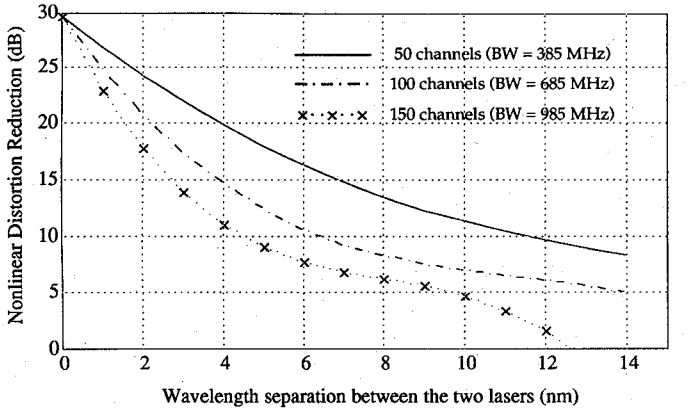

Fig. 3. Dispersion penalty as a function of wavelength separation between the two lasers. Fiber length = 10 km, fiber chromatic dispersion (at center wavelength) = 0.75 ps/nm · km.

IV. Noise Analysis

The noise analysis is divided into two parts. At first, we present a simplified analysis which does not take into account reduction of laser RIN by feedforward compensation. Following this analysis a theoretical investigation regarding the potential of a feedforward scheme to partially cancel out laser RIN and the implications on the system CNR are discussed.

Fig. 4 shows the dependence of the system's CNR on the optical coupling ratio used at the output of the linearized transmitter. In this analysis we have assumed a total received optical power of 0 dB, optical modulation depth (OMD) of 4%, a RIN figure of -155 dB/Hz for both lasers and preamplifier noise of 5 $pA/\sqrt{Hz}$. A possible RIN reduction was not taken into account here. As expected, the system's CNR is improved by coupling more light from L1 into the output signal, because the signal is modulated almost entirely on this laser. It is interesting to note that in case a coupling ratio of 50 : 50 is chosen, CNR specifications of about 50 dB for both linearized outputs can be met by utilizing low-intensity noise (< -155 dB/Hz) and high power sources (>5 dB) that enable the level of received optical power to be kept near 0 dB. For all other coupling ratios there exist only one linearized output signal.

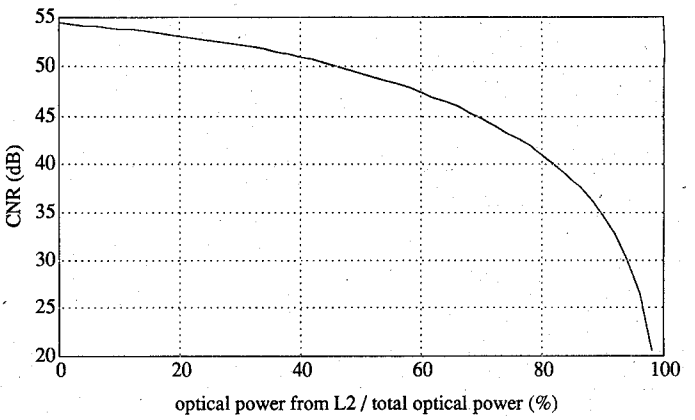

Fig. 4. CNR versus optical coupling ratio. Received optical power = 0 dBm, Optical Modulation Depth = 4%, RIN for both lasers = -155 dB/Hz, preamplifier noise = 5 $pA/\sqrt{Hz}$.

The additional advantage of a feedforward scheme is its potential to reduce relative intensity noise generated by the primary laser L1. This has been demonstrated by Fock and Tucker [8]. Even though a measured noise reduction of 10 dB was reported, no information was given about the coupling ratio of the optical coupler with which this result was achieved, nor what the tradeoff is, with respect to nonlinear reduction. The following discussion will show that in order to achieve noise reduction, nonlinear distortion reduction must be sacrificed.

Since the error signal is obtained by comparing the reference signal with a signal out of L1, it contains distortion products and noise introduced to the system by this laser. Therefore, by combining the "corrective" signal from L2 with the original signal from L1, a cancellation of distortion products, as well as that of intensity noise, can be achieved. Theoretically, the amount of linearization and improvement in intensity noise is limited by distortion and noise added to the system by L2. While the distortion from L2 is typically small because the error signal modulating this laser is small, the RIN added into the system may be relatively large depending on the choice of optical coupling ratio. This effect is illustrated in Fig. 5, which presents simulation results regarding the dependence of RIN reduction on the optical coupling ratio. We have assumed L1 and L2 have identical RIN figures. As might have been expected, the effect of RIN reduction is greatest (>20 dB) for low coupling ratios of laser L2. For a 50 : 50 coupling ratio, which is an attractive option for reasons explained before, the best possible RIN reduction is only 6 dB. It should be noted that the above results represent the best possible performance of the feedforward scheme. Practical results will again be limited by the device and component tolerances in the system and the above results

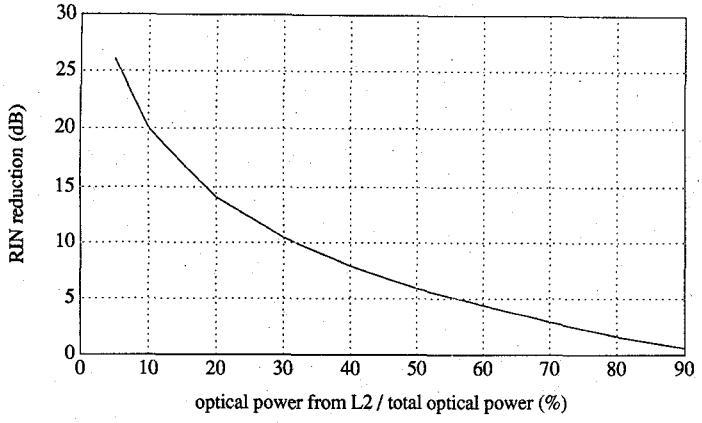

Fig. 5. RIN reduction versus optical coupling ratio.

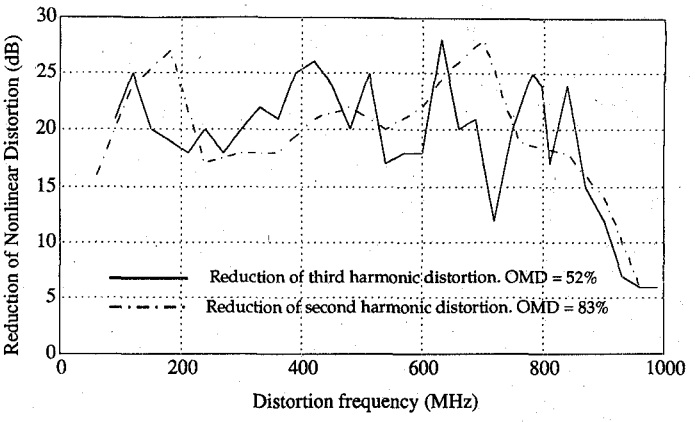

Fig. 7. Feedforward experimental results with one-tone tests.

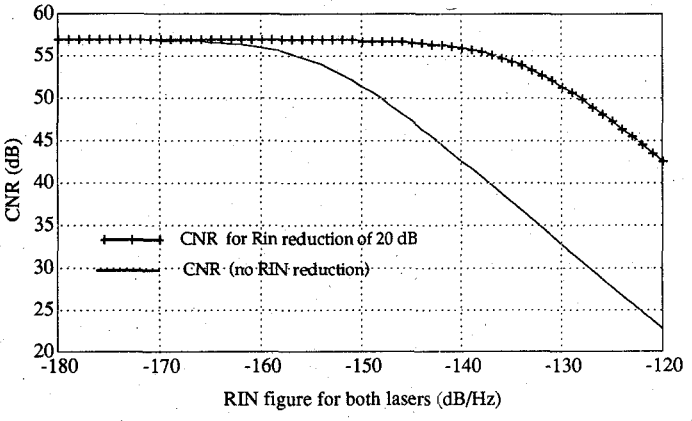

Fig. 6. CNR versus RIN figure (for both lasers), received optical power = 0 dBm, Optical Modulation Depth = 4%, Preamplifier noise = 5 $pA/\sqrt{Hz}$.

are expected to deteriorate further. In this context, it is also interesting to examine how a reduction in laser intensity noise affects the system CNR. Assuming a received optical power of 0 dBm, preamplifier noise of 5 $pA/\sqrt{Hz}$ and OMD of 4%, the CNR versus lasers RIN is plotted in Fig. 6. Two cases are presented in this figure; no RIN reduction and RIN reduction of 20 dB which represents the maximum available reduction at a coupling ratio of 90:10. It can be seen that for high RIN sources the improvement is substantial, while for low RIN lasers, only a marginal improvement is obtained. Thus, for example, a CNR improvement of 18.6 dB is obtained by using sources with RIN of -130 (dB/Hz), while an improvement of only 2.6 dB is achieved by using high quality DFB lasers with a typical RIN figure of -155 (dB/Hz). This results from the fact that at low RIN figures the dominant noise component is shot noise and not intensity noise. It is interesting to note that, at least theoretically, a CNR of 50 dB can be met by a feed forward transmitter, employing sources with a RIN figure of only -130 (dB/Hz).

V. Experimental Results

To verify the performance of the system we have used a pair of ASTROTEC 238 Type AT&T DFB lasers and EPITAXX low-distortion InGaAs photodiodes. An optical coupling ratio of 50:50 was chosen. The system was carefully optimized using a Wiltron 360B automatic vector network analyzer.

The circuit was tested by a series of one- and two-tone tests over a bandwidth of 1 GHz. Results regarding the reduction of second- and third-order harmonic distortion are given in Fig. 7. An average distortion reduction of 20 dB is achieved over a bandwidth of 850 MHz. Two-tone tests are shown in Fig. 8 which indicate also that the intermodulation distortion improvement was on the average about 20 dB over that frequency range. We have found that system bandwidth was mainly limited by the performance of the RF components being used in the circuit, especially the two 1 GHz RF amplifiers, which exhibit an increasing phase nonlinearity at frequencies above 800 MHz. Reduction of third-order intermodulation products of the type 2f1-f2 and 2f2-f1 was evaluated by a series of two-tone tests at optical modulation depth of 28% per tone. A typical linearization of 20 dB was obtained.

We have also performed an experimental investigation of the dispersion penalty on the system performance. The available linearization after transmission through 8.7 km of fiber was tested with a feedforward system which was optimized for transmission length of only a few meters. Dispersion penalty was typically found to be 1–2 dB at most distortion frequencies, except at the upper end of the bandwidth, where it reaches a maximum of 8 dB at 850 MHz. These findings agree well with our theoretical prediction. Based on our experimental results regarding one-tone and two-tones tests, and our simulation software, a prediction can be made regarding the system performance for a high (60–150) number of channels.

To measure noise cancellation the main transmitting laser L1 was replaced by a noisy BT&T Fabry-Perot laser (RIN -130 dB/Hz) while the ASTROTEC DFB laser

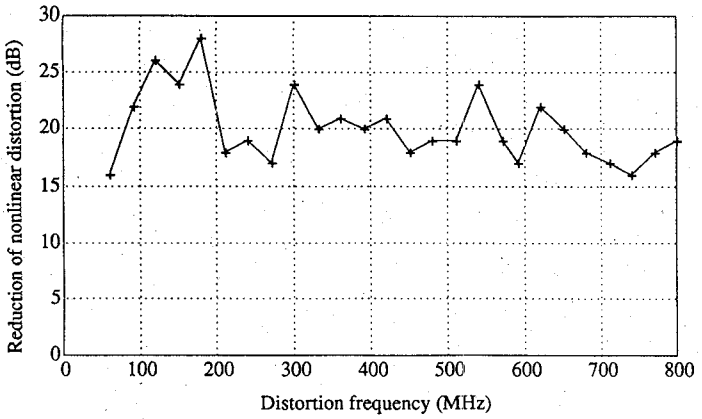

Fig. 8. Feedforward experimental results with two-tone tests (intermodulation distortion reduction).

was still employed as the correcting laser L2. Due to the significantly different characteristics of both lasers, the electrical and optical loop in the feedforward scheme had to be retuned. At the time of this publication we were only able to confirm the noise cancellation within a small frequency range of 20 MHz. With a coupling ratio of 50 : 50, a theoretical noise reduction of 6 dB was predicted while the measurements have shown a 3–4 dB improvement on the average.

VI. Conclusions

We have simulated and experimentally verified a feedforward linearization scheme for directly modulated analog lasers. Simulation results have been presented regarding the theoretical and practical limitations of this linearization scheme, as well as concerning dispersion penalty in the system. It was shown theoretically and experimentally that besides nonlinear distortion reduction a substantial reduction of laser intensity noise can be achieved as well. Thus it is possible to use higher RIN sources (lower cost lasers), while still satisfying the system CNR of better than 50 dB.

Appendix A

The following explains the derivation of the time varying part of (1). First, we note that both the applied current and photon density can be divided into ac and dc parts

$$I_a(t) = I_{dc} + I_{ac}(t) \tag{4}$$

$$Q(t) = Q_0 + q(t) \tag{5}$$

where I_{dc} is the laser's biasing current, $I_{ac}(t)$ is the modulating current, and Q_0 and $q(t)$ are the steady state and time varying parts of the photon density, respectively. Next, we substitute the denominator of the last term in (1) by its Taylor expansion around the steady state value. This is done in the following way:

$$\frac{1}{(1-\epsilon Q)Q} \cong f(Q_0) + f'(Q_0)\cdot q + f''(Q_0)\cdot q^2 + f'''(Q_0)\cdot q^3 \tag{6}$$

where

$$f(Q_0) = \frac{1}{(1-\epsilon Q_0)Q_0} \tag{7}$$

$$f'(Q_0) = \frac{2\epsilon Q_0 - 1}{(1-\epsilon Q_0)^2 Q_0^2} \tag{8}$$

$$f''(Q_0) = \frac{2(3\epsilon^2 Q_0^2 - 3\epsilon Q_0 + 1)}{(1-\epsilon Q_0)^3 Q_0^3} \tag{9}$$

$$f'''(Q_0) = \frac{6(4\epsilon^3 Q_0^3 - 6\epsilon^2 Q_0^2 + 4\epsilon Q_0 - 1)}{(1-\epsilon Q_0)^4 Q_0^4}. \tag{10}$$

Using the above expansions and the information given in (4) and (5), in (1), the following time varying equation is obtained:

$$\begin{aligned} I_{ac}(t) = {} & D\cdot q(t) + E\cdot q'(t) + F\cdot q''(t) \\ & + M\cdot\{q(t)\cdot q'(t)\} + N\cdot\{q'(t)\}^2 \\ & + N\cdot\{q''(t)\} \\ & + S\cdot\{q^2(t)\cdot q'(t)\} + 2G\cdot\{q(t)\cdot(q'(t))^2\} \\ & + G\cdot\{q^2(t)\cdot q''(t)\} \end{aligned} \tag{11}$$

D, E, F, M, N, S and G are all expressed by the laser parameters: Γ, τ_p, g, ϵ, V' and Q_0 in the following way

$$D = \frac{V'}{\Gamma\tau_p} \tag{12}$$

$$E = \frac{V'}{\Gamma}\left\{1 + \frac{f(Q_0) + Q_0\cdot f'(Q_0)}{\tau_p g}\right\} \tag{13}$$

$$F = \frac{V'}{\Gamma}\cdot\frac{f'(Q_0)}{g} \tag{14}$$

$$M = (-1)\cdot\frac{V'}{\Gamma\tau_p g}\{2\cdot f'(Q_0) + Q_0\cdot f''(Q_0)\} \tag{15}$$

$$N = (-1)\cdot\frac{V'}{\Gamma}\cdot\frac{f'(Q_0)}{g} \tag{16}$$

$$S = \frac{V'}{\Gamma g\tau_p}\cdot\left\{\frac{3\cdot f''(Q_0) + Q_0\cdot f'''(Q_0)}{2}\right\} \tag{17}$$

$$G = \frac{V'}{\Gamma}\cdot\frac{f''(Q_0)}{2g}. \tag{18}$$

Appendix B

The first three complex transfer functions of an inverse laser system are denoted as G_1, G_2 and G_3. They are given

by

$$G_1(\omega_1) = D + jE \cdot \omega_1 - F \cdot \omega_1^2 \tag{19}$$

$$G_2(\omega_1, \omega_2) = jM \cdot (\omega_1 + \omega_2) - N \cdot (\omega_1 + \omega_2)^2 \tag{20}$$

$$G_3(\omega_1, \omega_2, \omega_3) = j2S \cdot (\omega_1 + \omega_2 + \omega_3) - 2G \cdot (\omega_1 + \omega_2 + \omega_3)^2 \tag{21}$$

the parameters D, E, F, M, N, S and G are defined in appendix A. The first three complex transfer functions of a laser system are denoted as H_1, H_2 and H_3. They are given by

$$H_1(\omega_1) = \frac{1}{G_1(\omega_1)}. \tag{22}$$

$$H_2(\omega_1, \omega_2) = \frac{1}{2} \cdot \frac{G_2(\omega_1, \omega_2)}{G_1(\omega_1) \cdot G_1(\omega_2) \cdot G_1(\omega_1 + \omega_2)}. \tag{23}$$

$$H_3(\omega_1, \omega_2, \omega_3) = \frac{1}{6}\left\{\frac{G_3(\omega_1, \omega_2, \omega_3)H_1(\omega_1)H_1(\omega_2)H_1(\omega_3) - G_2(\omega_1 + \omega_2, \omega_3)Z}{G_1(\omega_1 + \omega_2 + \omega_3)}\right\} \tag{24}$$

where

$$Z \equiv H_1(\omega_1)H_2(\omega_2, \omega_3) + H_1(\omega_2)H_2(\omega_1, \omega_3) + H_1(\omega_3)H_2(\omega_1, \omega_2). \tag{25}$$

ACKNOWLEDGMENTS

The authors wish to thank U. Hielscher, visiting work-term student from the University of Stuttgart, Germany, and D. Grunow, Research Engineer in the LLiMiC group for retuning the feedforward system and performing the noise measurements.

REFERENCES

[1] T. Biswas and W. McGee, "Volterra series analysis of semiconductor laser diode," *IEEE Photon. Tech. Lett.*, vol. 3, no. 8, Aug. 1991, pp. 706–708.

[2] L. S. Foch, R. S. Tucker, and A. J. Lowery, "Linearization of analog-modulated semiconductor laser by feedforward compensation," in *Pro. Con. Lasers and Electro-Optics*, Baltimore, MD, May 1991, vol. 10, p. 378.

[3] K. Y. Lau and A. Yariv, "Intermodulation distortion in a directly modulated semiconductor injection laser," *Appl. Phys. Lett.*, vol. 45, no. 10, pp. 1034–1036, Nov. 1984.

[4] T. E. Darcie, R. S. Tucker, and G. J. Sullivan, "Intermodulation and harmonic distortion in InGaAsP laser," *Electron. Lett.*, vol. 21, no. 16, pp. 665–666, Aug. 1985, and "Errata" *Electron. Lett.*, vol. 22, no. 11, p. 619, May 1986.

[5] W. I. Way, "Large signal nonlinear prediction for single-mode laser diode under microwave intensity modulation," *lEEE Journ. Light. Tech.*, vol. LT-5, no. 3, pp. 305–315, March 1987.

[6] R. S. Tucker and I. P. Kaminow, "High-frequency characteristics of directly modulated InGaAsP ridge waveguide and buried heterostructure lasers," *IEEE Journ. Light. Tech.*, vol. LT-2, no. 4, pp. 385–393, Aug. 1984.

[7] P. Jannone and T. E. Darcie, "Multichannel intermodulation distortion in high-speed GaInAsP laser," *Electron. Lett.*, vol. 23, no. 25, pp. 1361–1362, Dec. 1987.

[8] L. S. Fock and R. S. Tucker, "Simultaneous reduction of intensity noise and distortion in semiconductor lasers by feedforward compensation," *Electron. Lett.*, vol. 27, no. 14, pp. 1297–1298, July 1991.

[9] S. A. Maas, *Nonlinear Microwave Circuits*, Artech House Inc., Norwood MA, 1988.

[10] E. Bedrosian and S. O. Rice, "The output properties of volterra systems (nonlinear systems with memory) driven by harmonic and Gaussian input," in *Proc. IEEE*, vol. 59, no. 12, pp. 1688–1707, Dec. 1971.

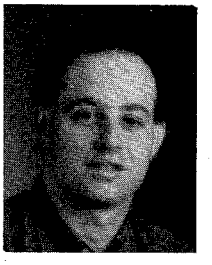

David Hassin received the B.Sc. degree in physics from the University of Tel-Aviv, Israel, in 1989. Currently, he is studying for the M.A.Sc. degree in electrical and computer engineering, at the University of Victoria, B.C., Canada, where he is involved in a research project regarding AM-SCM lightwave systems for CATV applications. His work in this project includes numerical modeling of laser diodes, simulation and analysis of various linearization schemes for optical transmitters as well as building and testing of a broadband feedforward linearization circuit for directly modulated laser transmitters.

Rüdiger Vahldieck (M'85–SM'86), for a photograph and biography, see this issue, p. 2255.